# EFFECTS OF THE AUGUST 11, 1999 TOTAL SOLAR ECLIPSE AS DEDUCED FROM TOTAL ELECTRON CONTENT MEASUREMENTS AT THE GPS NETWORK

E. L. Afraimovich, E. A. Kosogorov, O. S. Lesyuta
Institute of Solar-Terrestrial Physics SD RAS,
p. o. box 4026, Irkutsk, 664033, Russia
fax: +7 3952 462557; e-mail: afra@iszf.irk.ru

**Abstract**

We present the results derived from measuring fundamental parameters of the ionospheric response to the August 11, 1999 total solar eclipse. Our study is based on using the data from about 70 GPS stations located in the neighbourhood of the eclipse totality phase in Europe. The eclipse period was characterized by a low level of geomagnetic disturbance ($Dst$-variation from -10 to -20 nT), which alleviated significantly the problem of detecting the ionospheric response to the eclipse. Our analysis revealed a well-defined effect of a decrease (depression) of the total electron content (TEC) for all GPS stations. The delay between minimum TEC values with respect to the totality phase near the eclipse path increased gradually from 4 min in Greenwich longitude (10:40 UT, LT) to 8 min at the longitude 16° (12:09 LT). The depth and duration of the TEC depression were found to be 0.2-0.3 TECU and 60 min, respectively. The results obtained in this study are in good agreement with earlier measurements and theoretical estimates.

## 1 Introduction

Experimental observations of the ionosphere at the time of solar eclipses provide the source of information about the character of behavior of the various ionospheric parameters. Regular ionospheric effects of solar eclipses are fairly well understood. They imply an increase of effective reflection heights, a reduction in concentration in the F-layer maximum, and a decrease in total electron content

(TEC) in the ionosphere, which is typical of the transition to the nightside ionosphere (Cohen, 1984). The behavior of the above parameters can be modeled using appropriate ionospheric models (Stubbe, 1970; Boitman et al., 2000).

The main parameters of the ionospheric response are the value of the delay $\tau$ with respect to the eclipse totality phase, as well as its amplitude $A$ and duration $\Delta T$. Almost all publications devoted to the study of the ionospheric response to solar eclipses present estimates of these parameters. A knowledge of these values makes it possible to refine, in terms of the respective aeronomic ionospheric models, the time constants of ionization and recombination processes at different heights in the ionopshere.

The measurements of $\tau$ were made by analyzing the characteristics of the ionosphere-reflected radio signal at vertical-incidence soundings at a network of ionospheric stations (Marriott et al., 1969; Goncharov et al., 1982; Boitman et al., 2000) by measuring the frequency Doppler shift at vertical- and oblique-incidence soundings (Boitman et al., 2000). In the cited references, the value of $\tau$ was found to vary from 0 (Marriott et al., 1969) to 20 min, with the amplitude $A$ of a decrease in local electron density of order $9 \times 10^4$ cm$^{-3}$, and the response duration of about 1 hour (Boitman et al., 2000).

Similar measurements at an ionospheric station were made during the solar eclipse of September 23, 1987 in the south-eastern Asia (Cheng, 1992). The amplitude, delay and duration of the ionospheric response were found to be $0.3 \times 10^6$ cm$^{-3}$, 18 min and 1 hour 30 min, respectively. At the same time, measurements during the eclipse of October 24, 1995 in the same region provided an estimate of $\tau$ of about 80 min (Huang, 1999), $\Delta T = 1$ hour 20 min, and $A$ in excess of $1 \times 10^6$ cm$^{-3}$. The measurements of $f_0F2$ over the Scaramanga station during a partial solar eclipse of May 20, 1996 (Anastassiadis, 1970) give the value of $\tau$ of about 38 min. In paper Zherebtsov et al. (1998a), the delay time of the ionospheric response to the eclipse was between 25 and 30 min (at 300 km altitude).

Interesting results were obtained in observations of an annular solar eclipse of May 30, 1984 at the Millstone Hill incoherent scatter radar (Salah, 1986). A decrease in electron density with respect to the eclipse totality phase occurred in this case 20–30 min later, with $A = 4 \times 10^6$cm$^{-3}$, and $\Delta T = 2$ hours 15 min. However, facilities of this kind are too few to be extensively used in experiments during solar eclipses.

The ionospheric response to the March 9, 1997 total solar eclipse was investigated using a network of ionosondes (Zherebtsov et al., 1998b). For this event, the position of the minimum of the trough in the time dependence of electron density was shifted with respect to the time of maximum occultation of the solar disk by 10–15 min, with $A = 1 \times 10^5$ cm$^{-3}$, $\Delta T = 1$ hour 15 min.

A large amount of data was obtained by measuring the Faraday rotation of the plane of polarization of VHF signals of geostationary satellites (Klobuchar et al., 1970; Hunter et al., 1974; Davies,1980; Rama Rao, 1982; Essex, 1982; Deshpande, 1982; Singh, 1989). These measurements revealed the eclipse-induced effect of

a deep depression (decrease) in TEC with the amplitude $A$ varying from 2 to 14 TECU, and with a typical time of TEC depression and recovery of about several hours (the unit of measurement of TEC that is adopted in the literature corresponds to $10^{16}$ $^{-2}$). The spread in the values of $\tau$ was also found to vary over a wide range, from 5 to 40 min.

According to Klobuchar et al. (1970), for a total solar eclipse that occurred in spring (March 7, 1970), the amplitude $A$ was 11 TECU, $\Delta T = 2$ hours 44 min, and $\tau$ of order 33 min. For the total solar eclipse of February 16, 1980, the observations at Waltair (Singh, 1989) gave the following estimates: $A =$ 0.11 TECU, $\Delta T = 1$ hour, and $\tau = 20$ min. Essex et al. (1982) inferred that for the total solar eclipse of February 20, 1979, the values of $A$ and $\tau$ are 14 TECU and 33 min, respectively.

Hence a large body of experimental data do not permit us to make any reliable estimates of the basic parameters of the ionospheric response. One of the reason for such a great difference is attributable to the use of different methods of measurements which differ greatly by spatial and temporal resolution. However, the main reason is caused by dissimilar characteristics of the eclipse itself, by geophysical conditions of individual measurements, and by a large difference of the latitude, longitude and local time when experiments are conducted.

To obtain more reliable information about the behaviour of the ionosphere during an eclipse, it is necessary to carry out simultaneous measurements over a large area covering regions with a different local time. Furthermore, high spatial (of some tens of kilometres at least) and temporal (at least 1 min) resolution is needed. However, none of the above familiar methods meets such requirements.

The development of the global navigation system GPS and the creation, on its basis, of extensive networks of GPS stations (which at the end of 1999 consisted of no less than 600 sites), the data from which are placed on the INTERNET (Klobuchar, 1997), open up a new era in remote sensing of the ionosphere. At almost any point of the globe and at any time at two coherently-coupled frequencies $f_1 = 1575.42$ MHz and $f_2 = 1227.60$ MHz, two-frequency multichannel receivers of the GPS system are used to carry out high-precision measurements of the group and phase delay along the line o sight between the ground-based receiver and satellite-borne transmitters in the zone of reception. The sensitivity afforded by phase measurements in the GPS system permits irregularities to be detected with an amplitude of up to $10^{-3}$–$10^{-4}$ of the diurnal variation of TEC.

Afraimovich et al. (1998) were the first to use in a detailed analysis of regular ionopsheric effects measurements of TEC and its gradients for the total solar eclipse of March 9, 1997, using for this purpose the GPS interferometer at Irkutsk. Their results bear witness to significant changes occurring in the process of ion production in the ionosphere during the solar eclipse, simultaneously in a large volume of space with a radius of at least 300 km at 300 km altitude. The delay of a minimum TEC value with respect to the phase of totality is about 10 min, the depth of TEC depression varies from 1 to 3 TECU, and $\Delta T = 1$ hour 15 min.

Boitman et al. (2000) obtained a good agreement of these data, as well of measurements for several HF Doppler sounding paths with results of a numerical simulations using the ionosphere-plasmasphere coupling model (Krinberg, 1984). Unfortunately, during this eclipse the total shadow's path in 1997 was monitored by only few GPS stations; therefore, it was not possible to determine the spatial-temporal characteristics of the ionopsheric response.

According to the data from five GPS stations reported by Tsai and Liu (1999) for the solar eclipses of October 24, 1995 and March 9, 1997, the delay $\tau$ varied over a broad range, from 0 to 30 min, the amplitude $A$ was close to 7 TECU, and $\Delta T$ varied from 40 min to 1 hour.

A unique opportunity to exploit the potential of the GPS network was provided by the total solar eclipse of August 11, 1999. For this period of time, the INTERNET made available the data from at least 100 GPS stations located in Western and Central Europe within and near the totality path. A massive flow of publications on the various ionospheric effects of this eclipse should be forthcoming, based on the GPS data in conjunction with the data from other observing facilities. The objective of this paper is to determine the basic parameters of the ionospheric response to the August 11, 1999 total solar eclipse using these data.

General information about the eclipse, and a description of the experimental geometry are given in Section 2. The ionospheric response to the eclipse is discussed in Section 3 using the data from reference ionospheric station Chilton. The processing technique for the GPS network data, and results derived from analysing the ionospheric response of the August 11, 1999 solar eclipse in Europe are outlined in Section 4. Results obtained in this study are discussed in Section 5.

# 2 The geometry and general information of total solar eclipse AUGUST 11, 1999

The last solar eclipse in the 20–th century began in North Atlantic, and path of the Moon's shadow made first landfall in south-western England at 10:10 UT; the Sun at that time was at an angle of 45° over the eastern horizon. The centre line duration of total eclipse averaged 2 min, and the total eclipse was confined to a narrow corridor 103 km wide.

Fig. 1 shows a schematic map of the path of the Moon's shadow crossing parts of Western and Central Europe (the data from Espenak, 1999 were used in constructing this map). The centre line of eclipse at ground level is shown as a thick line, and thin lines correspond to its southern and northern boundaries. The location of reference ionospheric station Chilton (RAL) is marked by the symbol $\star$. Dots $\bullet$ and symbols + show the locations of the GPS stations used in the analysis; their geographic coordinates are presented in Table 1. Dots $\bullet$, together

with symbols + are used to represent a total set of GPS stations. Symbols + form a network of GPS stations located near the eclipse path; therefore, we designated this group as the near zone. Numbers for the longitudes $10°W$, $0°$, $10°E$, $20°E$, $30°E$, $40°E$ correspond to the local time for these longitudes.

In this paper we confine ourselves to analysing only to a region of Western and Central Europe from the coast of southern England to the point with coordinates $56.03°N$, $37.2°E$, where the totality phase was observed at 11:20 UT (14:20 LT). Thus the solar eclipse effect occurred for the conditions of the daytime summer ionosphere.

The distance along the great-circle arc between the above-mentioned extreme points is about 2900 km, with the time difference of 67 min only. Hence a distinguishing characteristic of this eclipse was the supersonic speed of the Moon's shadow sweeping through the terrestrial surface, exceeding 720 m/s.

At ionospheric heights the totality path was travelling somewhat further south. The onset time of the totality phase for the height h=300 km over Budapest is 1.3 min ahead of that at ground level. The difference in the values of the totality phases and their onset times is caused by the Sun's altitude over the horizon. At the time of the totality phase in Budapest (11:05 UT, or 14:05 LT), it was as small as 59°.

The period under consideration was characterized by a low level of geomagnetic disturbance ($Dst$-variation from -10 to -20 nT), which simplified greatly the problem of detecting the ionospheric response of eclipse.

# 3 The ionospheric response by eclipse from date of ionospheric station Chilton

First we consider the variations of critical frequencies $f_0F2$ over the time interval 00:00-24:00 UT on August 11, 1999 according to the data from station Chilton (RAL) - Fig. 2a. The onset time of the totality phase of eclipse in the area of station Chilton (RAL) at 300 km altitude is shown by a vertical solid line. As might be expected under the conditions of the summer ionosphere, the mean level of $f_0F2$ differs only slightly for the night-time and daytime. Nevertheless, a decrease of $f_0F2$ during the totality phase of eclipse is sufficiently clearly distinguished.

Consider the variations of ionospheric parameters for the time interval 06:00–15:00 UT on August 11, 1999, and on the background days of August 10 and 12, using the data from station Chilton (RAL) - Fig. 3. Dots correspond to variations of critical frequencies $f_0F2$ (panel a), $f_0F1$ (panel c), apparent heights $h'F$ (panel b), and $h'F2$ (panel d) for August 11, 1999. Solid curves plot the same values that are smoothed with a time window of 60 min. For August 10 and 12, only smoothed curves are given, with the same time window of 60 min.

The onset time of the totality phase of eclipse (10:16 UT) at 300 km altitude over the station is shown by a thin vertical line.

The eclipse effect is most conspicuous in the variations of critical frequencies $f_0F2$, whose maximum difference from the background values on August 10 and 12 at the time of reaching a minimum (10:20 UT) was up to 2 MHz. On the other hand, the amplitude of a decrease of $f_0F2$ for the August 11 event (after the totality phase of eclipse) does not exceed 1 MHz. The eclipse effect on other parameters is not as clearly distinguished, and becomes evident only when comparing the smoothed curves. Similar results of measurements at an ionospheric station were obtained during the total solar eclipse of September 23, 1987 in South-Eastern Asia (K. Cheng, 1992).

The $f_0F2$ – variations, measured at station Chilton (RAL) at time intervals of 4 min, are presented in greater detail in Fig. 4a (heavy dots). The solid curve connecting these dots is an approximating one for these values. This panel plots also the geometrical function of eclipse $S(t)$ at 300 km altitude, calculated for station Chilton. Minimum values of $f_0F2$ and $S(t)$ correspond to the points A and B in this figure. The respective delay $\tau$ between the time of a minimum of $f_0F2$ and of the function $S(t)$ is close to 4 min in this case.

The data from the station Chilton (RAL) and from GPS station HERS nearest to it are compared in the next Section.

# 4 The process of GPS–network data and results of analysis of ionospheric effect by total solar eclipse of August 11, 1999

We now give a brief account of the sequence of procedures used in processing the GPS data. Input data are represented by series of "oblique" values of TEC $I(t)$, as well as by the corresponding series of elevations $\theta(t)$ measured from the ground, and azimuths $\alpha(t)$ of the line of sight to the satellite measured clockwise from the northward direction. These parameters are calculated by our developed CONVTEC program by converting the GPS-standard RINEX-files from the INTERNET. Series of elevations $\theta(t)$ and azimuths $\alpha(t)$ of the line of sight to the satellite are used to determine the location of subionospheric points. In the case under consideration, all results were obtained for larger than 45° elevations $\theta(t)$.

Fig. 4c presents the experimental geometry in the area of ionospheric station Chilton (RAL) - $\star$, and GPS station HERS ($\bullet$). Heavy dots $\bullet$ show the centre line of eclipse at ground level, and smaller dots correspond to its southern and northern boundaries. The symbol $*$ shows the position of the subionospheric point at the time of a maximum response of TEC (see below).

Various methods for reconstructing the absolute value of TEC are currently under development using measurements of both phase and group delays; however,

effective algorithms for an accurate solution of this problem are still unavailable for the different types of two-frequency receivers and operating modes of the GPS system. In this connection, for purposes of this paper, we limit our attention to considering only those TEC variations which were obtained from phase delay measurements by formula (Afraimovich et al., 1998):

$$I_p = \frac{1}{40.308} \frac{f_1^2 f_2^2}{f_1^2 - f_2^2} [(L_1\lambda_1 - L_2\lambda_2) + const + nL] \quad (1)$$

where $L_1\lambda_1$ and $L_2\lambda_2$ are additional paths of the radio signal caused by the phase delay in the ionosphere, (m); $L_1$ and $L_2$ represent the number of phase rotations at the frequencies $f_1$ and $f_2$; $\lambda_1$ and $\lambda_2$ stand for the corresponding wavelengths, (m); *const* is the unknown initial phase ambiguity, (m); and $nL$ are errors in determining the phase path, (m).

For an approximate specification of the TEC constant component $I_0$ at time intervals of 2 hours, we made use of the INTERNET data on corresponding global maps of the absolute vertical value of TEC in the IONEX format (Mannucci, 1998) - see also Fig. 2b. To normalize the response amplitude we converted the "oblique" TEC to an equivalent "vertical" value:

$$I(t) = I_p(t) sin(\theta(t)) \quad (2)$$

Although, because of a strong horizontal TEC gradient and without regard for the spericity of the problem, this procedure gives a very rough result, but this result is quite acceptable because all our results were obtained for larger than 45° elevations $\theta(t)$.

With the purpose of eliminating variations of the regular ionosphere, as well as trends introduced by the satellite's motion, we employ the procedure of eliminating the trend by preliminarily smoothing the initial series with the time window in the range from 40 to 100 min which is fitted for each TEC sampling. Such a procedure is also required for a clearer identification of the ionospheric response of eclipse which is characterized by a relatively small amplitude (see below) under the presence of space-time TEC variations that are not associated with the eclipse.

For the purposes of illustration of the data processing procedure Fig. 5 presents the filtered TEC variations $dI(t)$ for August 11 (thick line), and for the background days of August 10 and 12, 1999 (thin lines) for station HERS for satellite N14 (PRN 14) - c), as well as for stations ZIMM (PRN 1) - b) and WTZT (PRN 14) - a), which are separated from station HERS, respectively, by 7° and 13° in longitude eastward. Figures correspond to GPS satellite numbers. The onset time of the totality phase of eclipse at 300 km altitude for the corresponding subionospheric points is shown by vertical solid lines. As is evident from the figure, responses to the eclipse at these stations are very similar in both form and amplitude, but the response delay increases with the longitude. $dI(t)$

– variations for the background days of August 10 and 12, 1999 for different stations differ substantially not only from the TEC response to eclipse but also from one another.

Fig. 4b presents the filtered variations of TEC $dI(t)$ for station HERS for PRN 14 during August 11, 1999 (thick line). This panel plots also the geometrical function of eclipse at 300 km altitude, $S(t)$, that is calculated for the subionospheric point of PRN 14. A minimum value of $S(t)$ corresponds to the point A in the figure.

As is apparent from this figure, the form of the filtered variations is similar to a triangle whose vertex (point B) corresponds to the time at which the TEC attains its minimum value. The value of $dI_{min}$ itself can serve as an estimate of the amplitude of TEC response to eclipse, and the time interval between the times of intersection of the line $dI$=0 (points C and D) can serve as an estimate of the duration of the response $\Delta T$. The corresponding delay $\tau$ between the times of the minimum of $dI_{min}$ and of the function $S(t)$ in this case was found to be 4 min, which coincides with the estimate of $\tau$ for ionospheric station Chilton (see Section 3). The response amplitude in this case was close to 0.18 TECU, and the response duration was 46 min.

Such $dI(t)$ – variations are characteristic for all GPS stations and satellite numbers 01 and 14 listed in Table 1. The choice of the same satellites, PRN 01 and PRN 14, for the entire selected set of GPS stations was dictated by the fact for these satellites a maximum value of the elevation $\theta$ of the line of sight to the satellite exceeded 45° for the time interval 10:00-12:30 UT, which reduced to a minimum the possible error of conversion to the "vertical" value of TEC as a consequence of the sphericity.

The first line of Table 2 presents the results of a statistical processing for the entire set of GPS stations listed in Table 1. The second line includes only those stations whichlie in the immediate vicinity of the eclipse path, within $\pm$ 5° with respect to the centre line (near zone). In Table 2, the values before the bar are mean values, and those after the bar correspond to the standard deviation. The mean value of $\tau$ for the entire set of stations is 16 min, while for the stations in the near zone this value is 7 min. The mean value of the amplitude A=0.3 TECU for all stations and A=0.1 TECU for the near zone. The width of the TEC trough for the far and near zones $\Delta T$ = 60 min, on average.

Fig. 6 presents a longitudinal dependence of the time position $t_{min}$ of minima of the curves $dI(t)$ for subionospheric points lying in the immediate vicinity of the eclipse band (satellites 1 and 14) - heavy dots. Dark symbols $\triangle$ designate the times of totality phases of the geometrical function of eclipse versus longitude which are calculated for the subionospheric points. Shaded symbols $\diamond$ correspond to delay times between maximum of the geometrical function of eclipse and a minimum in TEC.

It was found that the delay $\tau$ increases gradually from 4 min at the Greenwich longitude (10:23 UT, LT) to 16 min at the longitude of 16° (12:09 LT).

# 5 Conclusions

Our results are in good agreement with earlier measurements and theoretical estimates (see a review of the data in the Introduction). The key feature of our data is a higher reliability of determining the main parameters of the response to eclipse which is due to high space-time resolution and to the increased sensitivity of detection of ionospheric disturbances inherent in the GPS-array method which we are using.

Also, due regard must be had to the fact that the distinctive property of the eclipse under consideration was a relatively small response amplitude, which required special filtering of the TEC series (see preceding Section). The reason is that, unlike a number of eclipses for which more-or-less reliable data were obtained, this eclipse occurred in the summer season characterized by only moderate differences of the daytime and night-time ionization. Furthermore, in this situation the time variation of $f_0F2$ and vertical TEC near noon usually shows a minimum which, in essence, masks the eclipse effect (see also Fig. 2b). It is also vital to note that the time constant of a decrease in ionization in the $F_2$ maximum exceeds substantially the duration of the totality phase of eclipse, which leads also to a decrease in response amplitude.

The local time-dependence of $\tau$ that is revealed in this paper is in agreement with theoretical estimates reported in (Stubbe, 1970). The value of $\tau$ for foF2, approaching 6 min, corresponded to 13:40 LT. Using modeling methods (Ivelskaya et al., 1977) showed that the variations of the delay time $\tau$ of minimum local electron density $N_e(t)$ with respect to a minimum of the ion production function are as follows: $\tau$ = 1-2 min at 150 km altitude, $\tau$ = 3 min at 200 km, $\tau$ = 20 min at 300 km, and $\tau$ = 45 min above 600 km. In this paper $\tau$ is estimated, respectively, at about 3 min for 200 km altitude and 20 min for 300 km altitude for 12 LT.

# 6 Acknowledgements

We are grateful to K. S. Palamartchouk, A. V. Tashchilin and A. D. Kalikhman for their interest in this study, helpful advice and active participation in discussions. Thanks are also due to V. G. Mikhalkosky for his assistance in preparing the English version of the manuscript. This work was done with support from the Russian foundation for Basic Research (grant 99-05-64753) and RFBR grant of leading scientific schools of the Russian Federation No. 00-15-98509.

# References

[1] Afraimovich E. L., Palamartchouk K. S., Perevalova N. P., and Chernukhov V. V., 1998. Ionospheric effects of the solar eclipse of March 9, 1997, as deduced from GPS data. Geophysical Research Letters, 25, 465–468.

[2] Rama Rao P. V. S., 1982. TEC observations at Waltair during the total solar eclipse of 16 february 1980 . Proc. Indian Nat. Sci. Acad., 48, 434–438.

[3] Klobuchar J. A., and Malik C., 1970. Comparison of changes in total electron content along three paths. Nature, 226, 1113–1114.

[4] Hunter A. N., Holman B. K., Fieldgate D. G. and Kelleher R., 1974. Faraday rotation studies in Africa during the solar eclipse of June 30, 1973. Nature, 250, 205–206.

[5] Essex E. A., Klobuchar J. A., Philbrick C. R. and Leo R., 1982. Response the total electron content of the ionosphere over North America to the total solar eclipse of 26 February, 1979. Proc. Indian Nat. Sci. Acad., 48, 444–457.

[6] Anastassiadis M. and Matsoukas D., 1970. Electron content measurements by beacon S-66 satellite during May 20, 1966 solar eclipse. Journal of Atmospheric and Solar-Terrestrial Physics, 34, 695–712.

[7] Boitman O. N., Kalikhman A. D. and Tashchilin A. V., 2000. The midlatitude ionosphere during the total solar eclipse of March 9, 1997. Journal Geophysical Research (accepted).

[8] Marriott R. T., John D. E. St., Thorne R. M., Venkateswaran S. V., and Mahadevan P., 1972. Ionospheric effects of two recent solar eclipses. Journal of Atmospheric and Solar-Terrestrial Physics, 31, 695–712.

[9] Kang Cheng, Yinn-Nien Huang, Sen-Wen Chen. Ionospheric Effects of Solar Eclipse of September 23, 1987, Around the Equatorial Anomaly Crest Region // Journ. Geophys. Res. 1992. V. 97. N 3. P. 103–111.

[10] Klobuchar J. A., 1997. Real-time ionospheric science: The new reality. Radio Science, 32, 1943–1952.

[11] Cohen E. A., 1984. The study of the effect of solar eclipses on the ionosphere based on satellite beacon observations. Radio Science, 19, 769–777.

[12] Davies K., 1980. Recent progress in satellite radio beacon studies with particular emphasis on the ATS-6 radio beacon experiment. Space Science Review, 25, 357–430.

[13] Espenak F. and Anderson J., 1999. Total solar eclipse of 1999 August 11, NASA Reference Publicftion 1398 // 1999. http://sunearth.gsfs.nasa.gov/eclipse/TSE1999/TSE1999.html.

[14] Krinberg I. A. , Tashilin A. B., 1984. Ionosphera and plasmasphera. Moscow: Nauka, p.189.

[15] Stubbe P., 1970. The F region during an eclipse – theoretical study. Journal of Atmospheric and Solar-Terrestrial Physics, 32, 1109–1116.

[16] Singh L., Tyagi T. R., Somayajulu Y. V. et al., 1989. A multi-station satellite radio beacon study of ionospheric variations during total solar eclipses. Journal of Atmospheric and Solar-Terrestrial Physics, 51, 271–278.

[17] Ivelskaya M. K., Sutyrina G. E. and Sukhodolskaya V. E., 1977. Modeling the solar eclipse effect in the ionosphere by different methods of specifying the electron temperature. Issledovaniya po geomagnetizmu, aeronomii i fizike Solntsa, 41, Moscow: Nauka, 62–65.

[18] Deshpande M. R., Chandra H., Sethia G. et al., 1982. Effects of the total solar eclipse of 16 February 1980 on TEC at low latitudes. Proc. Indian. Nat. Sci. Acad., part A, 48, Suppl. N 3., 427–433.

[19] Goncharov L. P. and Sitnov Yu. S. 1982. Solar eclipse effects over Cuba. Ionosfer. prognoz., Moscow, 169–171.

[20] Salah J. E., Oliver W. L., Foster J. C. et al., 1986. Observations of the May 30, 1984, annular solar eclipse at Millstone Hill. Journal Geophysical Research, part A, 91, 1651–1660.

[21] Huang C. R. and Liu C. H., 1999. A study of tomographically reconstructed ionospheric images during a solar eclipse. Journal Geophysical Research, 104, 79–94.

[22] Mannucci A. J., Ho C. M., Lindqwister U. J. et al., 1998. A global mapping technique for GPS-drived ionospheric TEC measurements. Radio Science, 33, 565–582.

[23] Zherebtsov G. A., Medvedev A. V., Potekhin A. P., and Shpynev B. G., 1998a. Ionospheric effects during the March 9, 1997 solar eclipse as deduced from observations at the Irkutsk incoherent scatter radar. Issledovaniya po geomagnetizmu, aeronomii i fizike Solntsa, 109, part 1, 46–50.

[24] Zherebtsov G. A., Klimenko V. V., Klimenko V. I. et al., 1998b. An investigation of the March 9, 1997 solar eclipse effect in the Asian part of Russia. Issledovaniya po geomagnetizmu, aeronomii i fizike Solntsa, 109, part 1, 51–54.

[25] Tsai H. F. and Liu J. Y., 1999. Ionospheric total electron content response to solar eclipses. Journal Geophysical Research , 104, 657–668.

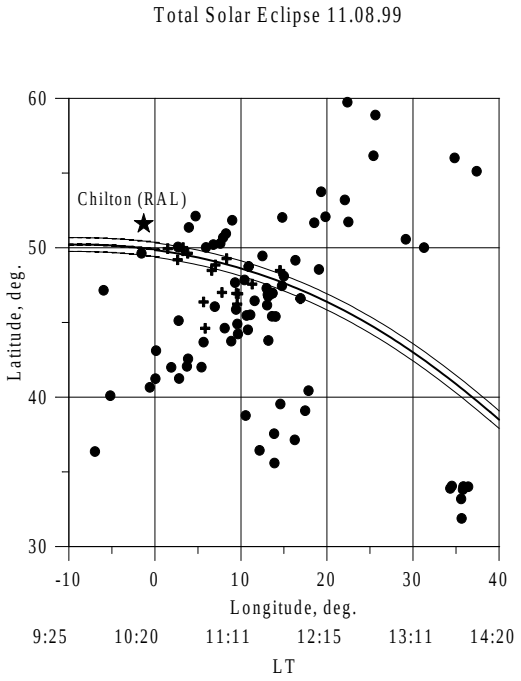


Fig. 1: Schematic map of the Moon's shadow sweeping through parts of Western and Central Europe. The centre line of eclipse at ground level is shown as a thick line, and thin lines correspond to the southern and northern boundaries. The symbols + and • designate the locations of GPS stations - their entire set (these stations were used in calculating the parameters appearing in the first line of Table 2). The symbols + correspond to the near zone (the stations of this group were used in calculating the parameters appearing in the second line of Table 2). The location of ionospheric station Chilton (RAL) is shown by $\star$. Numbers for the longitudes $10^\circ W$ $0^\circ$, $10^\circ E$, $20^\circ E$, $30^\circ E$, $40^\circ E$ designate the local time for these longitudes.

Table 1: GPS site names and locations

| N | SITE | Geograph. latitude | Geograph. longitude | | N | SITE | Geograph. latitude | Geograph. longitude |
|---|---|---|---|---|---|---|---|---|
| 1 | BELL | 41.600 | 1.401 | | 29 | MADR | 40.429 | 4.250 |
| 2 | BOR1 | 52.277 | 17.073 | | 30 | MATE | 40.649 | 16.704 |
| 3 | BRST | 48.380 | -4.496 | | 31 | MDVO | 56.027 | 37.223 |
| 4 | BRUS | 50.798 | 4.359 | | 32 | MEDI | 44.520 | 11.647 |
| 5 | BSHM | 32.779 | 35.023 | | 33 | MEEU | 51.106 | 5.556 |
| 6 | BZRG | 46.499 | 11.337 | | 34 | MEMB | 50.590 | 5.977 |
| 7 | CAGL | 39.136 | 8.973 | | 35 | METS | 60.217 | 24.395 |
| 8 | COSE | 39.201 | 16.310 | | 36 | MOPI | 48.372 | 17.274 |
| 9 | CREU | 42.319 | 3.316 | | 37 | NOTO | 36.876 | 14.990 |
| 10 | DENT | 50.934 | 3.400 | | 38 | OBER | 48.086 | 11.280 |
| 11 | DOUR | 50.095 | 4.595 | | 39 | PATK | 47.208 | 11.460 |
| 12 | EBRE | 40.821 | 0.492 | | 40 | PFAN | 47.515 | 9.785 |
| 13 | GENO | 44.419 | 8.921 | | 41 | RAMO | 30.598 | 34.763 |
| 14 | GILB | 32.479 | 35.416 | | 42 | RIGA | 56.949 | 24.059 |
| 15 | GLSV | 50.364 | 30.497 | | 43 | SBGZ | 47.803 | 13.110 |
| 16 | GOPE | 49.914 | 14.786 | | 44 | SFER | 36.464 | 6.206 |
| 17 | GRAA | 47.067 | 15.493 | | 45 | SJDV | 45.879 | 4.677 |
| 18 | GRAS | 43.755 | 6.921 | | 46 | TELA | 32.068 | 34.781 |
| 19 | GRAZ | 47.067 | 15.493 | | 47 | TORI | 45.063 | 7.661 |
| 20 | HERS | 50.867 | 0.336 | | 48 | TOUL | 43.561 | 1.481 |
| 21 | HFLK | 47.313 | 11.386 | | 49 | UPAD | 45.407 | 11.878 |
| 22 | JOZE | 52.097 | 21.031 | | 50 | VENE | 45.437 | 12.331 |
| 23 | KABR | 33.022 | 35.145 | | 51 | WARE | 50.690 | 5.245 |
| 24 | KARL | 49.011 | 8.411 | | 52 | WSRT | 52.915 | 6.604 |
| 25 | KATZ | 32.995 | 35.688 | | 53 | WTZR | 49.144 | 12.879 |
| 26 | KOSG | 52.178 | 5.810 | | 54 | WTZT | 49.144 | 12.879 |
| 27 | LAMA | 53.892 | 20.670 | | 55 | ZIMM | 46.877 | 7.465 |
| 28 | LAMP | 35.500 | 12.606 | | | | | |

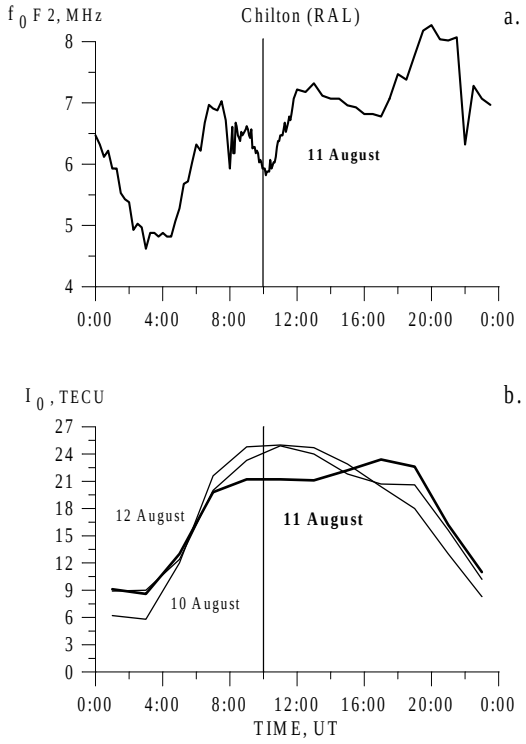


Fig. 2 : **a)**Variations of the critical frequencies $f_0F2$ over the time interval 00:00-24:00 UT on August 11, 1999 according to the data from station Chilton (RAL). **b)** Variations of the absolute vertical value of TEC for the same time interval of August 11, 1999 (thick line), and for the background days of August 10 and 12 (thin lines) - see text. The onset time of the totality phase of eclipse at 300 km altitude is shown by a vertical solid line.

Table 2 : The ionospheric parameters of total solar eclipse of august 11, 1999

| N | Number of subionospheric points | A, TECU | $\Delta T$, min | $\tau$, min |
|---|---|---|---|---|
| 1 | 98 | 0.298 / 0.197 | 62 / 32 | 16.4 / 14 |
| 2 | 19 | 0.193 / 0.081 | 61 / 36 | 8 / 4 |

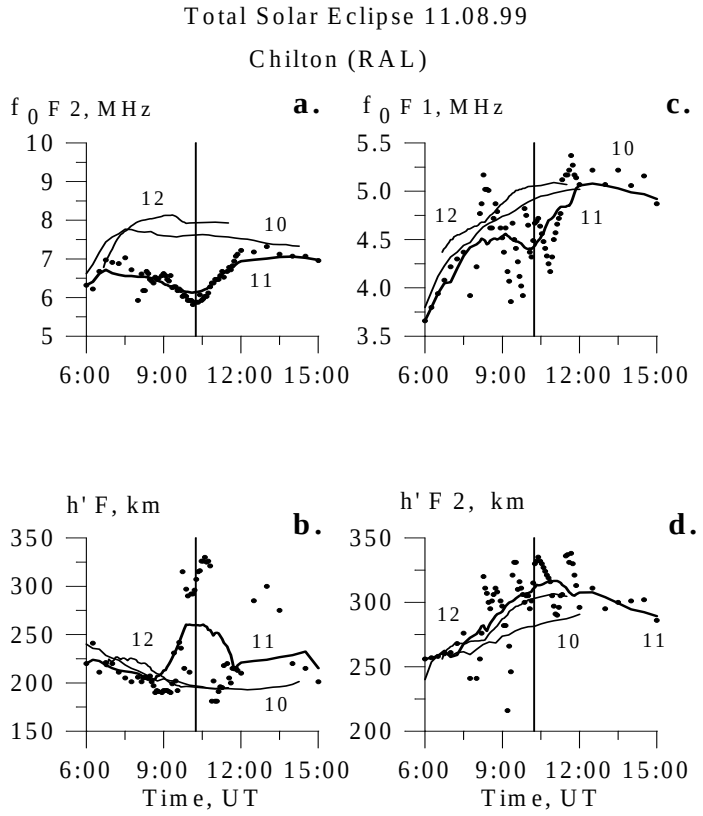


Fig. 3 : Variations of ionospheric parameters during 06:00-15:00 UT on August 11, 1999 and on the background days of August 10 and 12, based on the data from station Chilton (RAL). Dots designate the variations of critical frequencies $f_0F2$ (panel a), $f_0F1$ (panel c), apparent heights $h'_F$ (panel b), and $h'_{F2}$ (panel d). Solid curves correspond to the same values, but smoothed with the time window of 60 min (only smoothed curves are given for August 10 and 12). The onset time of the totality phase of eclipse at 300 km altitude is shown by a vertical solid line.

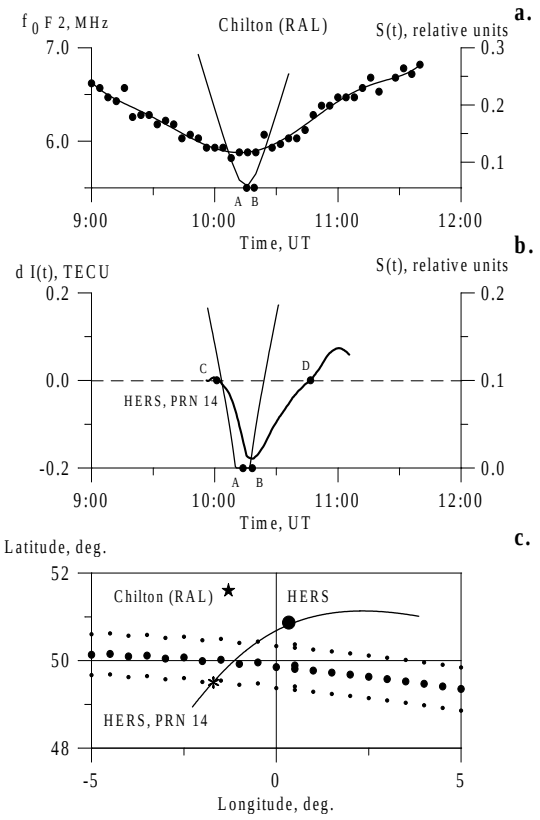


Fig. 4 : **a)** Values of the critical frequency $f_0F2$, measured on August 11, 1999 at station Chilton (RAL) at time intervals of 4 min during 09:00-12:00 UT (dots). The solid curve connecting these dots is an approximating one for these values. This panel plots also the geometrical function of eclipse at 300 km altitude, $S(t)$, calculated for station Chilton. **b)** Filtered variations of the total electron content dI(t) for station HERS (PRN 14) for August 11, 1999 - the thick line. This panel plots also the geometrical function of eclipse at 300 km altitude, $S(t)$, calculated for the subionospheric point of PRN 14. **c)** Experimental geometry in the area of ionospheric station Chilton (RAL) - $\star$, and for GPS station HERS ($\bigcirc$). Heavy dots show the center line of eclipse at ground level, and smaller symbols $\cdot$ show the southern and northern boundaries. The symbol $*$ shows the position of the subionospheric point at the time of a maximum response of TEC.

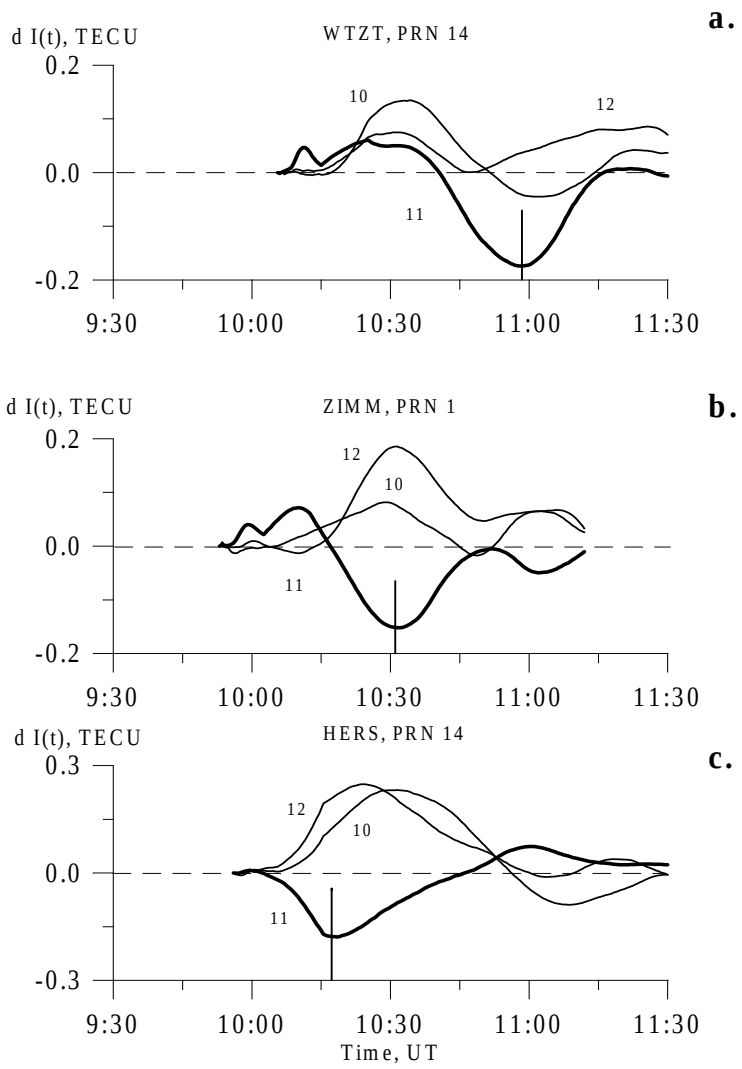


Fig. 5 : Filtered variations of the total electron content $dI(t)$ for August 11 (thick line), and for the background days of August 10 and 12, 1999 (thin lines) for station HERS - a), ZIMM - b), and WTZT - c). Figures correspond to the GPS satellite numbers. The onset time of the totality phase of eclipse at 300 km altitude for corresponding subionospheric points is shown by vertical solid lines.

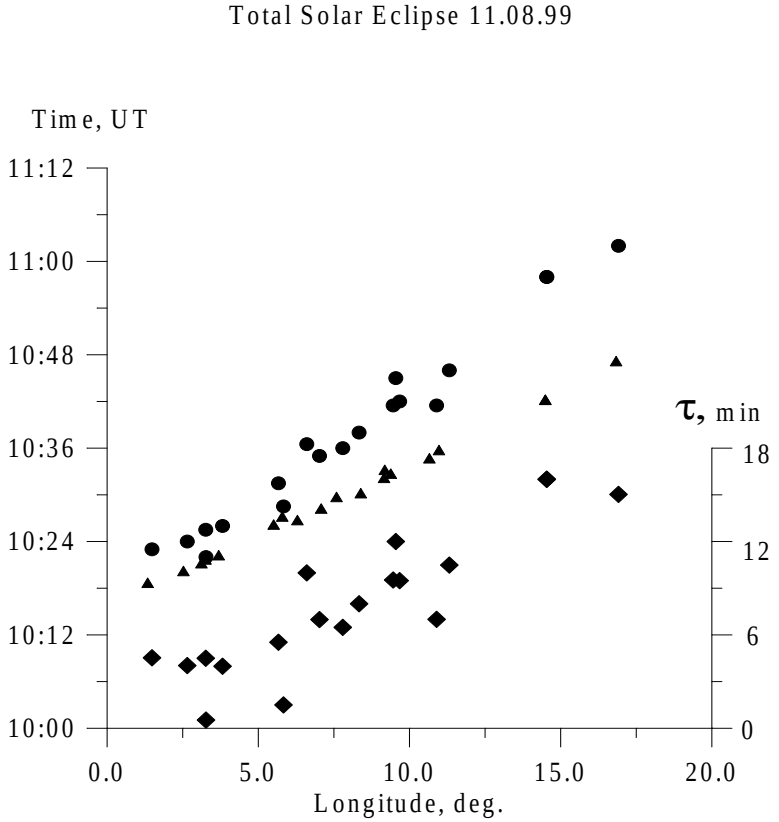


Fig. 6 : Longitudinal dependence of the time position of minima of the curve $dI(t)$ for the stations in the near zone - heavy dots •. The symbols △ designate the variations of the totality phase of eclipse at 300 km altitude for subionospheric points as a function of longitude. The symbols ⋄ plot the longitudinal dependence of the delay $\tau$ of the TEC response $dI(t)$.